AIAA JOURNAL
Vol. 30, No. 3, March 1992

Models of Space-Averaged Energetics of Plates

O. M. Bouthier* and R. J. Bernhard†
Purdue University, West Lafayette, Indiana 47907

The analysis of high-frequency vibrations of plates is of particular interest for many cases of structure-borne noise in aircraft. The current methods of analysis are either too expensive (finite element method) or may have a confidence band wider than desirable (statistical energy analysis). An alternative technique to model the space- and time-averaged response of structural acoustics problems with enough detail to include all significant mechanisms of energy generation, transmission, and absorption is highly desirable. The focus of this paper is the development of a set of equations that govern the space- and time-averaged energy density in plates. To solve this equation, a boundary value problem must be considered in terms of energy density variables using energy and intensity boundary conditions. A verification study of the energy governing equation is performed. A finite element formulation of the new equations is also implemented and several tests cases are analyzed and compared to analytical solutions.

Nomenclature

c_g = group speed of bending wave in plates
D = bending stiffness of the plate
E = Young's modulus
e = energy density, J/m^2
e_j = energy density at a node in the FEM formulation
F = force amplitude
$[F]$ = vector of f_i
h = thickness of the plate
j = $\sqrt{-1}$
$[K]$ = matrix of k_{ij}
$[P]$ = vector of p_i
q = intensity vector, W/m
$q(x, y)$ = vibrational power input to the plate
w = transverse displacement of the plate
w_{ff} = far-field component of w
π_{diss} = power dissipated in the plate
ϕ = Lagrangian interpolation functions
$[\Psi]$ = matrix of m_{ij}
η = loss factor
ν = Poisson's ratio
ρ = mass per unit area of the plate
ω = circular frequency
$\int_D$ = integral over the domain of the plate
$\int_\Gamma$ = integral around the boundary of the plate
∇ = del operator
$\langle x \rangle$ = time average of the variable x
$\bar{x}$ = space average of the variable x

Introduction

THE vibration of machines at high frequencies is of significant concern to engineers in the field of aircraft interior noise and vibration control. In most applications, the energy of vibration flows in the structure and is eventually radiated as unwanted sound in inhabited spaces. In high-speed aircraft, engine vibration and turbulent flow around the fuselage and wings excite the structure and cause noise. To control structure-borne noise, it is desirable to understand the paths along which energy travels from its source through a structure to the inhabited space of interest.

The dynamic response of structures is sensitive to the frequency of the excitation and to the position at which the response is being observed. The sensitive dependence on frequency and position of the response is particularly hard to quantify at high frequencies due to the fuzzy nature of system properties and boundary conditions. Thus, at high frequency, overall system performance and characteristics are best evaluated on a space and frequency average basis. A robust and efficient technique of analyzing the global response of structures in the mid- to high-frequency range is desirable.

In the past, various methods for the analysis of vibration have been used to solve problems of structure-borne noise in aircraft.[1-4] At low frequencies, the finite element method is useful and reliable.[5,6] At high frequencies however, the finite element method becomes too expensive and manpower intensive.[7] At frequencies where modal density is high, statistical energy analysis (SEA) is a useful tool to determine the global behavior of built-up structures.[8] SEA, however, does not provide information about the variation of the response within components of a built-up structure nor is it straightforward to model local subsystem damping treatments. As modal density decreases, the confidence band of SEA predictions may become larger than desirable.

The goal of this investigation is to develop a set of governing differential equations that predict the energy density and intensity in a space- and time-averaged sense for plates. A parallel investigation for the flow of energy in beams and rods has been conducted by Wohlever.[9,10] Independent research in the field of wave propagation in rods has been conducted by Lase and Jezequel[11] and by Nefske and Sung.[12] The analysis proposed here takes into account the local absorption of energy due to internal damping and also predicts the intensity field in plates. Simple cases are used to test the energy governing equations in order to compare the results to those obtained from Lagrangian plate theory. A finite element formulation of the energy governing equations is developed and implemented to solve more complex problems.

Derivation of Energy Governing Equations for the Plate

Although the analysis presented in this paper restricts itself to plates in applications, the general procedure described in this section has been shown to apply to rods, beams, and membranes as well.[9,12] From continuum mechanics, the en-

Presented as Paper 90-3921 at the AIAA Aeroacoustics Conference, Tallahassee, Florida, Oct. 22-24, 1990; received Feb. 5, 1991; revision received July 3, 1991; accepted for publication July 9, 1991.

*Research Assistant, School of Mechanical Engineering, Ray W. Herrick Laboratories.

†Professor, School of Mechanical Engineering, Ray W. Herrick Laboratories. Member AIAA.

ergy distribution in a structure must obey conservation principles, which can be stated in equation form as[13]:

$$\frac{\partial e}{\partial t} = -\nabla \cdot \boldsymbol{q} - \pi_{\text{diss}} \tag{1}$$

For steady-state conditions, the time derivative term in Eq. (1) is zero and Eq. (1) becomes:

$$\nabla \cdot \boldsymbol{q} = -\pi_{\text{diss}} \tag{2}$$

Various models of energy dissipation in elastic media are discussed in the literature. For the analysis presented here, an approximate hysteresis damping model is used. Cremer and Heckl show how the power dissipated in the medium is related to the reversible energy density in the medium in such a way that[14]

$$\pi_{\text{diss}} = \eta\omega e \tag{3}$$

Eq. (3) is a good approximation of energy dissipation if the energy lost within one cycle is small compared to the reversible energy density.

For thermal and fluid systems, it is generally true that energy flows from locations of high energy density to locations of low energy density. In equation form, such behavior is modeled by an energy transmission relationship of the form

$$\boldsymbol{q} \propto -\nabla e \tag{4}$$

When Eqs. (2), (3), and the relationship in (4) are combined, an energy relation can be written as

$$\nabla^2 e \propto \eta\omega e \tag{5}$$

The relationship in Eq. (5) is a second-order expression that can be formulated numerically and used to model the behavior of energy in relatively complex systems. It would be desirable if similar equations could be found to model energy distributions in structures.

Except for rods, structures do not behave according to Eq. (4) in a strict sense as shown by Wohlever.[9] The primary task of this investigation is to find a relationship between energy density and intensity that can be used with Eqs. (2) and (3) to develop an energy density governing equation. The derivation of this energy transmission relationship and the subsequent energy density equation depend on certain assumptions and restrictive conditions that are documented here. The derivation of the equations derived here can be found in the literature[12] but will be shown here, for completeness.

The Lagrange equation of motion for a thin, transversely vibrating plate excited harmonically in time by a point force at (x_0, y_0) is:

$$D_c\nabla^4 w + \rho\frac{\partial^2 w}{\partial t^2} = F\delta(x - x_0)\delta(y - y_0)e^{j\omega t} \tag{6}$$

where

$$D_c = \frac{E_c h^3}{12(1 - \nu^2)} \tag{7}$$

where $E_c = E(1 + j\eta)$. The complex form of Young's modulus is often used to introduce damping in elastic media by effectively making propagating plane waves decay exponentially as a function of distance.[14]

For the analysis presented here, the far-field harmonic solution of the homogeneous form of Eq. (6) is used:

$$w_{ff}(x, y, t) = (A_1 e^{-jk_x x} + B_1 e^{jk_x x})(A_2 e^{-jk_y y} + B_2 e^{jk_y y})e^{j\omega t} \tag{8}$$

where k_x and k_y are the x and y components of the complex wave number, respectively. Because the stiffness of the plate in Eq. (6) is complex, the wave number is also complex. The usefulness of the far-field solution for the analysis of vibrating plates at medium- to high-frequencies was shown by Noiseux.[15] If k_{x1} and k_{y1} are the real parts of k_x and k_y respectively, then

$$(k_{x1}^2 + k_{y1}^2)^2 = \omega^2\frac{\rho}{D} \tag{9}$$

For small damping, k_x and k_y are well approximated by

$$k_x = k_{x1}\left(1 - j\frac{\eta}{4}\right) \qquad k_y = k_{y1}\left(1 - j\frac{\eta}{4}\right) \tag{10}$$

The energy in plates is transmitted by shear forces (Q_x and Q_y), bending moments (M_x and M_y), and twisting moments (M_{xy} and M_{yx}). These forces and moments are related to the transverse displacement as

$$M_x = -D\left(\frac{\partial^2 w}{\partial^2 x} + \nu\frac{\partial^2 w}{\partial^2 y}\right)$$

$$M_y = -D\left(\frac{\partial^2 w}{\partial^2 y} + \nu\frac{\partial^2 w}{\partial^2 x}\right) \tag{11a}$$

$$Q_x = -D\frac{\partial}{\partial x}\left(\frac{\partial^2 w}{\partial^2 x} + \frac{\partial^2 w}{\partial^2 y}\right)$$

$$Q_y = -D\frac{\partial}{\partial y}\left(\frac{\partial^2 w}{\partial^2 y} + \frac{\partial^2 w}{\partial^2 x}\right) \tag{11b}$$

$$M_{xy} = D(1 - \nu)\frac{\partial^2 w}{\partial x\partial y} \qquad M_{yx} = -M_{xy} \tag{11c}$$

The expression for the x component of intensity is

$$q_x = Q_x\frac{\partial w}{\partial t} - M_x\frac{\partial^2 w}{\partial x\partial t} + M_{xy}\frac{\partial^2 w}{\partial y\partial t} \tag{12}$$

The expression for the y component of intensity is similar to Eq. (12).

Expressions for the potential and kinetic energy in the plate can also be found in the literature.[16] The total energy density e in the plate

$$e = \frac{D}{2}\left[\left(\frac{\partial^2 w}{\partial x^2}\right)^2 + \left(\frac{\partial^2 w}{\partial y^2}\right)^2 + 2\nu\frac{\partial^2 w}{\partial x^2}\frac{\partial^2 w}{\partial y^2} + 2(1 - \nu)\frac{\partial^2 w}{\partial x\partial y}\right] + \frac{\rho}{2}\left(\frac{\partial w}{\partial t}\right)^2 \tag{13}$$

is the sum of the potential energy and the kinetic energy.

Only the steps involved in the derivation of an energy transmission relationship will be described here because the algebraic manipulations involved are lengthy. Substitution of Eq. (8) into Eq. (12) yields an expression for the x component of intensity in terms of the constants A_1, A_2, B_1, and B_2. The y component of intensity can be obtained in a similar manner. Substitution of Eq. (8) into Eq. (13) yields an expression for the energy density in the plate in terms of the constants A_1, A_2, B_1, and B_2. These expressions for intensity and energy density are time averaged. The energy and intensity expressions are simplified by neglecting all terms of order η^2 and higher. However, no obvious relationship between energy and intensity is apparent at this stage. The energy and intensity equations are further simplified by neglecting all the terms containing sinusoidal functions of the wavenumber. This sim-

plification is the equivalent to conducting a space averaging of the form:

$$\langle \bar{e} \rangle = \frac{k_{x1}k_{y1}}{4\pi^2} \int_0^{2\pi/k_{x1}} \int_0^{2\pi/k_{y1}} \langle e \rangle \, dx \, dy$$

$$\langle \bar{q} \rangle = \frac{k_{x1}k_{y1}}{4\pi^2} \int_0^{2\pi/k_{x1}} \int_0^{2\pi/k_{y1}} \langle q \rangle \, dx \, dy$$

The reduced expressions for the energy density and the intensity components are relatively simple functions of A_1, A_2, B_1, and B_2. These expressions are shown in the Appendix. A brief examination of the equations in the Appendix reveals that the simplified expressions for energy density and intensity are related in the following manner:

$$\langle \bar{q} \rangle_{ff} = -\frac{c_g^2}{\eta\omega} \nabla \langle \bar{e} \rangle_{ff} \tag{14}$$

It is of particular interest to note that the intensity is a function of the group speed even on a space averaged basis. Using Eqs. (2) and (3) with the transmission equation. Eq. (14), the energy equation for the far-field space and time averaged energy density becomes

$$\frac{c_g^2}{\eta\omega} \nabla^2 \langle \bar{e} \rangle_{ff} - \eta\omega \langle \bar{e} \rangle_{ff} = 0 \tag{15}$$

Eq. (15) is a differential equation that models the time and space averaged far-field energy density in plates. Eqs. (14) and (15) have also been shown to be valid for various types of waveguides, such as rods, beams, and membranes, if the appropriate group speed is used.[12] Due to the choice of variables in this analysis (energy density and intensity), it may be possible to distinguish between certain boundary conditions. For instance, the gradient of the energy density normal to the edge of a plate vanishes it the edge is simply supported or free. This approximation is a trade-off for the simplicity of the solution of Eq. (14) and (15).

Equation (15) can be solved either analytically or numerically. Energy and intensity boundary conditions must be enforced for the solution of Eq. (15). The solution of problems using Eq. (15) will result in predictions of time- and (locally) space- averaged far-field energy variables. The shortcomings of the predictions made by Eq. (15) in the near field are shown in the next section. Note that Eq. (15) is not a two-dimensional Helmholtz equation.

Analytical Solutions

In this section the analysis of a simply supported vibrating square plate excited by pressure distributed over a small area (see Fig. 1) is performed using a Fourier series expansion solution technique to find the displacement solution. Energy density and intensity are found by using Eqs. (12) and (13), respectively. The results are compared to solutions obtained by solving Eqs. (14) and (15) using Fourier Series techniques.

The plate used for these verification studies is a simply supported plate 1 m × 1 m × 1 mm in dimension and made of aluminum. The plate excitation is such that the force is constant over the frequency band from 20 Hz to 64 Hz. For this frequency bandwidth excitation location, we can show that at least eight modes are being excited. The solutions for all frequencies are summed to give the energy density and intensity distributions in the frequency band. The energy density in the plate calculated from classical plate theory is shown in Fig. 2. The x and y components of intensity from the classical solution are shown in Fig. 3. The vector representation of Fig. 3 is shown in Fig. 4.

The same problem was solved using Eqs. (14) and (15) and a Fourier series technique. The boundary conditions are such that no intensity flows normal to the edges of the plate at the supports (see Fig. 5). The input power amplitude, q_{in}, is calculated from the "exact" solution of the plate vibrating at 42 Hz (the center frequency of the frequency band mentioned above). The energy density solution of Eq. (15) is shown in Fig. 6. The x and y components of intensity are shown separately in Fig. 7. The vector representation of Fig. 7 is shown in Fig. 8.

The plots of intensity shown in Fig. 4 show some energy circulation in the plate. The intensity field shown in Fig. 8 shows no evidence of circulation of energy anywhere in the plate because of the space-averaged nature of the results obtained from Eqs. (14) and (15). However, the intensities pre-

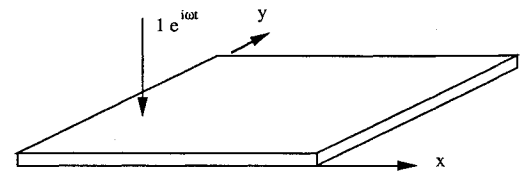

Fig. 1 Plate with local pressure excitation.

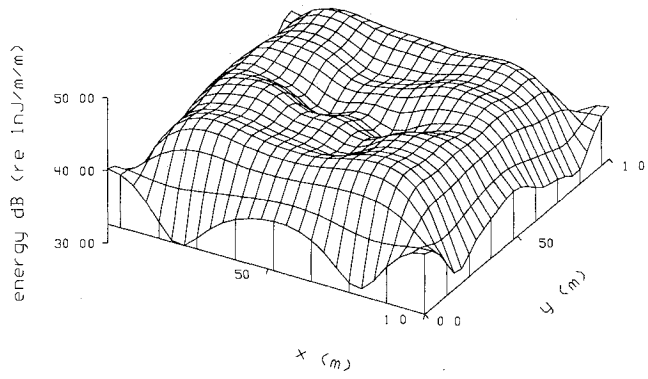

Fig. 2 "Exact" energy density.

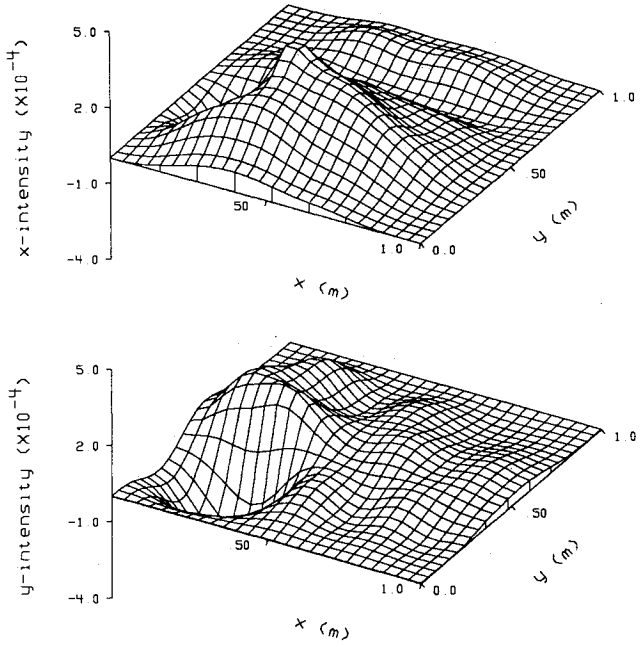

Fig. 3 x and y components of the "exact" intensity field.

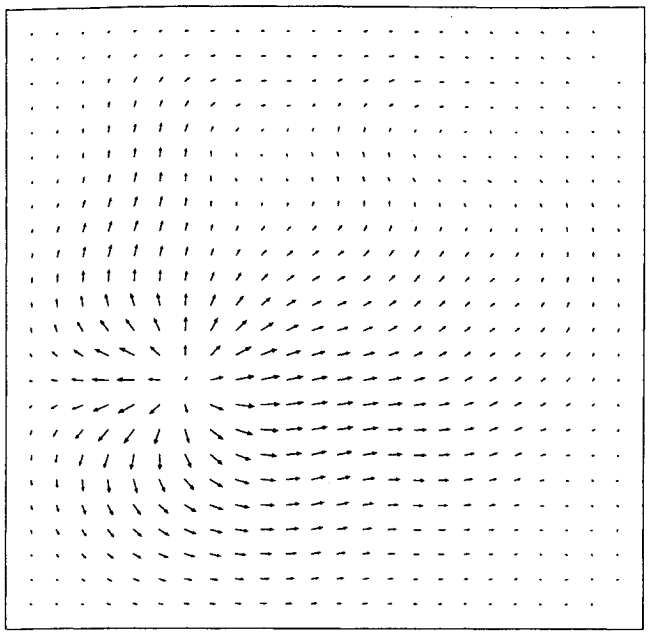

Fig. 4 "Exact" intensity field. The maximum vector is $5 \cdot 10^{-4}$ W/m.

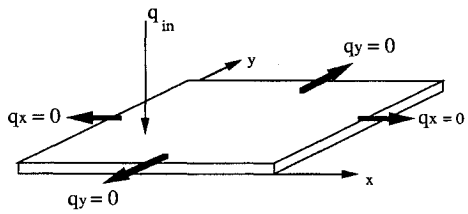

Fig. 5 Plate with local power input.

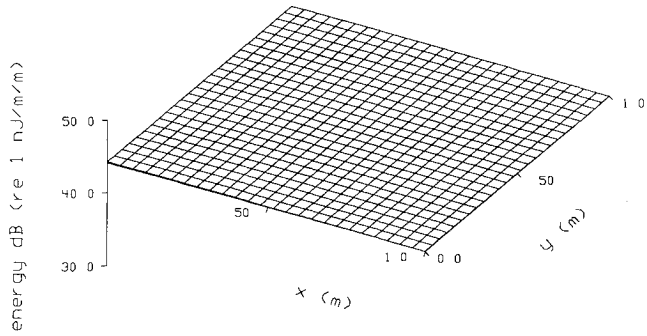

Fig. 6 Approximate energy density solution.

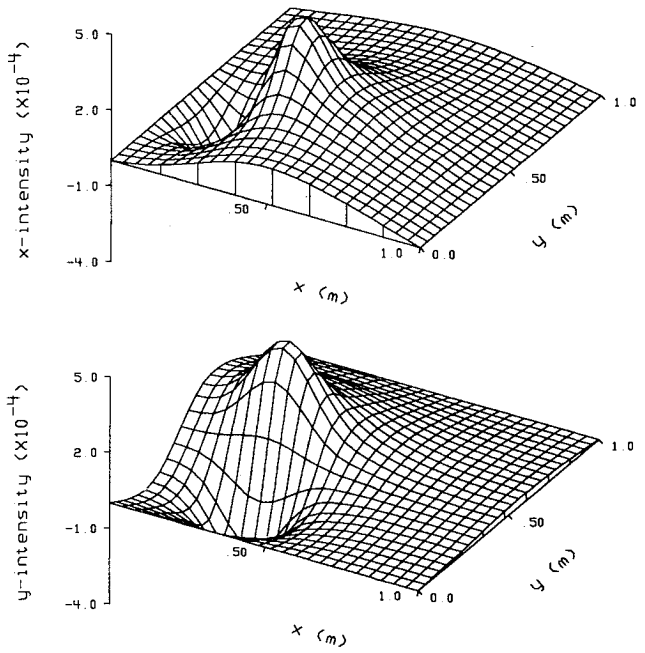

Fig. 7 x and y components of the approximate intensity field.

dicted by the two schemes presented here are generally well matched.

The energy density predicted by the approximate scheme of Eqs. (14) and (15) is a good average of the energy density calculated from the classical theory. The "exact" response shown in Fig. 2 is rough compared to the approximate response shown in Fig. 6 because the frequency band considered for the simulation shown in Fig. 1 includes relatively few modes (44 Hz). When the modal density is higher, the "exact" response becomes smoother and the approximate solution matches the exact solution even more closely shown in Figs. 2 and 6. The average energy density level in Fig. 2 is 43.9 dB and the average energy density level in Fig. 6 is 44.8 dB.

Finite Element Formulation

In this section, a finite element formulation of Eq. (15) is developed and used to solve several vibrating plate examples. There are many advantages to be gained by formulating the energy governing equations via the finite element method. When Eq. (15) is implemented numerically, the parameters $c_g^2/\eta\omega$ and $\eta\omega$ are not required to be constants. The damping, Young's modulus, and the thickness of the plate can be functions of position. In addition, the behavior of plates with complex geometry can be predicted.

The finite element formulation of Eq. (15) is illustrated here for the general problem where external energy is input:

$$\frac{c_g^2}{\eta\omega}\nabla^2 e - \eta\omega e + q(x, y) = 0 \qquad (16)$$

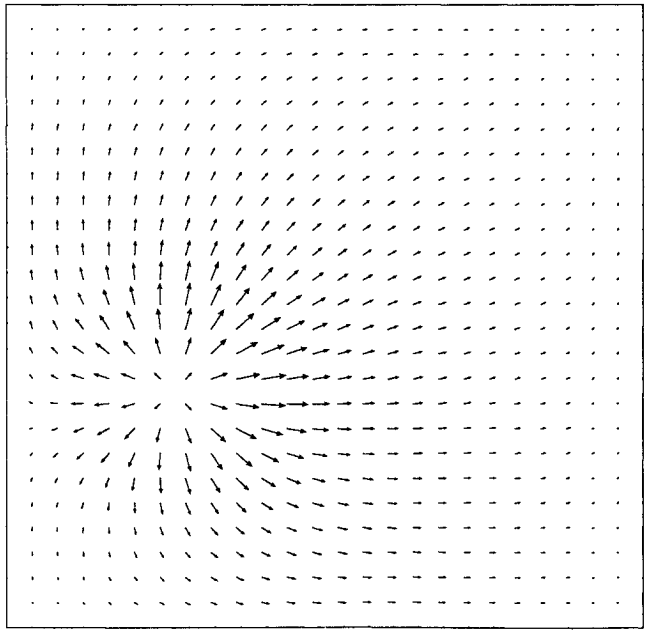

Fig. 8 Approximate intensity field. The maximum vector is $5 \cdot 10^{-4}$ W/m.

where $q(x, y)$ is the input power. From the theory of finite element analysis,[17] the weak form variational statement of Eq. (16) can be written as

$$\int_D \nu\left(\frac{c_g^2}{\eta\omega}\nabla\cdot\nabla e - \eta\omega e + q\right) dD = \int_\Gamma \nu\left(n\cdot\frac{c_g^2}{\eta\omega}\nabla e\right) d\Gamma - \int_D \frac{c_g^2}{\eta\omega}\nabla\nu\cdot\nabla e\, dD - \int_D \eta\omega e\nu\, dD + \int_D \nu q\, dD = 0 \quad (17)$$

where ν is a trial function used in the variational procedure that leads to the finite element formulation of the problem. For a Galerkin weighted residual scheme using quadratic elements, the following approximation is made:

$$e = \sum_{j=1}^{9} e_j\Phi_j \quad (18)$$

and

$$\nu = \Phi_i \quad (19)$$

Substituting Eqs. (18) and (19) into Eq. (17) yields the following equation:

$$p_i - \sum_j e_j k_{ij} - \sum_j e_j m_{ij} + f_i = 0 \quad (20)$$

The terms in Eq. (20) are defined as

$$k_{ij} = \int_D \frac{c_g^2}{\eta\omega}\nabla\Phi_i\cdot\nabla\Phi_j\, dD$$

$$m_{ij} = \int_D \eta\omega\Phi_i\Phi_j\, dD$$

$$f_i = \int_D q\Phi_i\, dD$$

$$p_i = \int_\Gamma \frac{c_g^2}{\eta\omega}\Phi_i(n\cdot\nabla e)\, d\Gamma$$

p_i represents the flux of energy across the boundary. The resulting element matrix equation is

$$[K + \Psi^2 M]e = [P + F] \quad (21)$$

The terms in Eq. (21) are evaluated using Gaussian quadrature numerical integration techniques frequently used in finite element methods. The global matrix equation is obtained by assembling the individual element matrix equations in a method described by Zienkiewicz.[18]

Finite Element Examples

To model the problem shown in Fig. 5 using the finite element method, the domain of the plate is modeled using 25 rectangular elements. Each element is defined by 9 nodes. The system model contains a total of 121 degrees of freedom. The physical properties of the plate are the same as those used in the analytical solution section.

The energy distribution of the vibrating plate shown in Fig. 5 of the previous section is solved using the finite element method (FEM). The excitation frequency is 42 Hz. The energy density solution is shown in Fig. 9. The FEM answers agree with the results shown in Figs. 2 and 6. The corresponding intensity field in the plate is shown in Fig. 10. The intensity fields shown in Figs. 8 are 10 are in good agreement (note that the plots are shown on the same scale). This example serves to show that the FEM can be used to accurately solve Eq. (15).

One last example is shown here to demonstrate the potential use of the finite element implementation of Eqs. (14) and (15) as a design tool. Consider the problem shown in Fig. 11. The power input into the plate is unevenly distributed, as shown in Fig. 11. The input power distribution is intended to

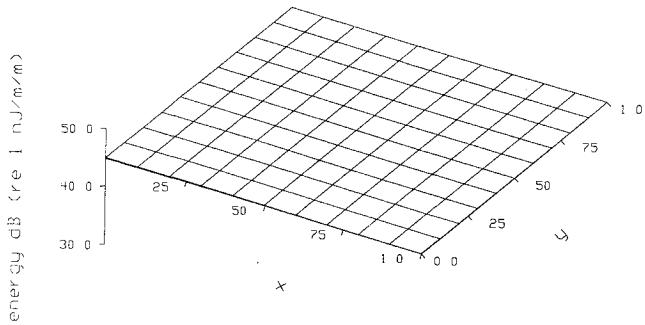

Fig. 9 FEM solution of the energy density.

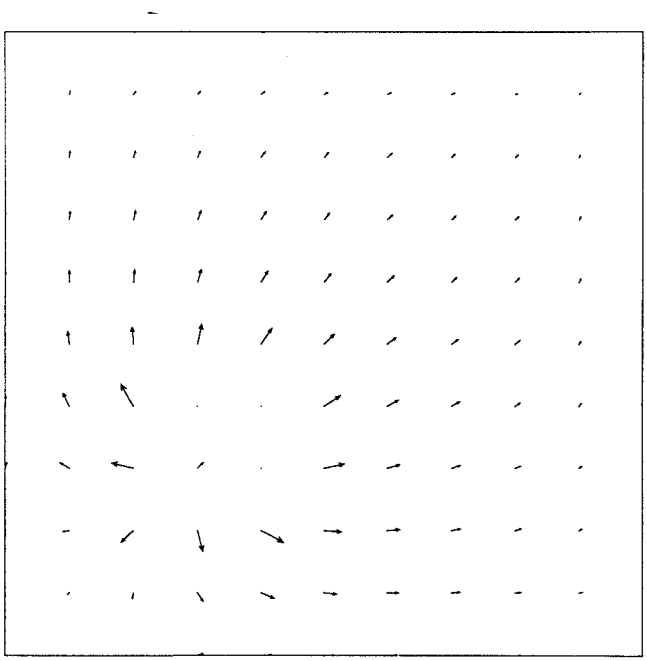

Fig. 10 FEM solution of the intensity field. The maximum vector is $5 \cdot 10^{-4}$ W/m.

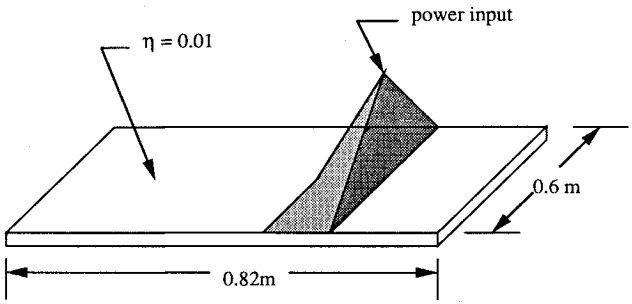

Fig. 11 Plate with a pressure excitation.

be similar to the type of power distribution encountered in a prop plane or due to turbulent fluid flow around a fuselage. The thickness of the plate is 1 mm. The plate is homogeneous and the loss factor is constant throughout the domain of the plate. The energy density solution is shown in Fig. 12. Although the energy distribution is fairly uniform, the scale in Fig. 12 has been expanded to show that the energy level at the power source is greatest and decays elsewhere in the plate. The energy density level of the plate obtained by using SEA is 56.2 dB. This result closely matches with the average of the energy distribution shown in Fig. 12.

As a second case study, the problem discussed above is slightly modified in such a way that the plate is now treated with strips with higher loss factors as shown in Fig. 13. The stiffness of the plate is still constant. The power input to the plate is unchanged. The corresponding energy level is shown in Fig. 14. The variation in energy density is more noticeable than in the first case. An energy drop can be observed within the damping treated strips, which is not surprising.

The third case study is shown in Fig. 15. The area of the plate in which the power is input is now treated with a coating of higher loss material while group speed properties are left unchanged. The corresponding energy distribution is shown in Fig. 16.

All these cases are shown simultaneously in Fig. 17. Note that in each case of this example, the energy density in the plate is reduced as the amount of lossy material increases. Note also, as shown in Figs. 14 and 16, that the gradient of energy density is greatest where the loss factor is greatest. The latter phenomenon is due to the fact that more energy per unit area is dissipated where the loss factor is high, which creates a high flux of energy into high loss regions.

The intensity fields for each case study of this example are shown in Fig. 18 from top to bottom for the order discussed above. In each case, the energy flows away from the power input area and is dissipated within the plate. Note, in the last case of Fig. 18, that some of the energy leaves the center of the region in which the power is input and circulates back to the outside of the high loss region. The reason for this behavior can be explained by the fact that a great amount of energy can be dissipated in the area of the power input. There-

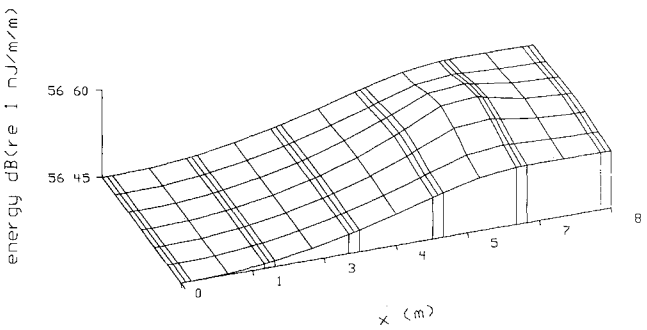

Fig. 12 Energy density in the plate shown in Fig. 11.

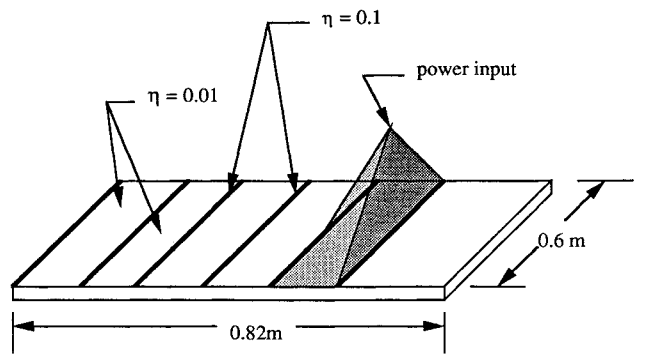

Fig. 13 Plate with a pressure excitation and damping strips.

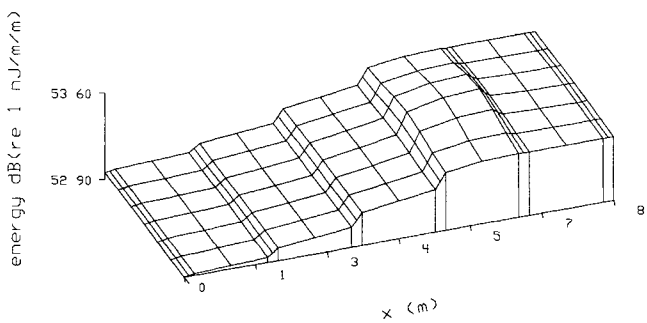

Fig. 14 Energy density in the plate shown in Fig. 13.

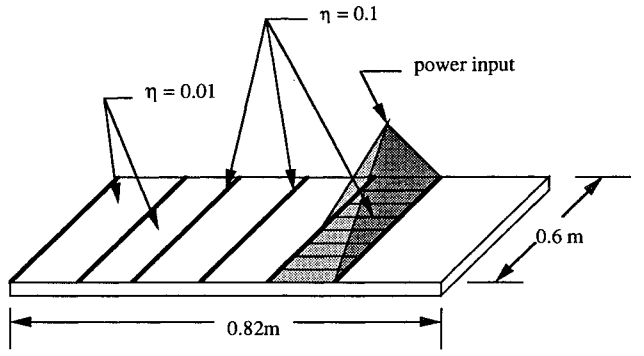

Fig. 15 Plate with a pressure excitation, damping strips, and a damping pad at the excitation location.

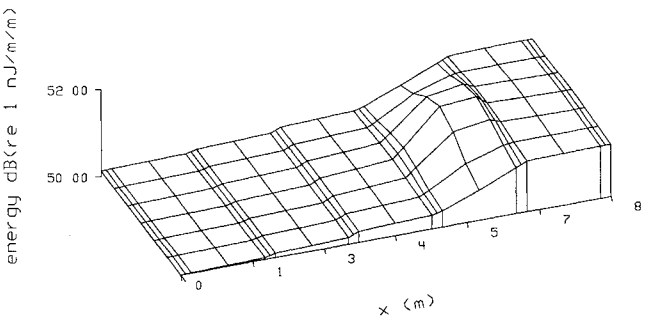

Fig. 16 Energy density in the plate shown in Fig. 15.

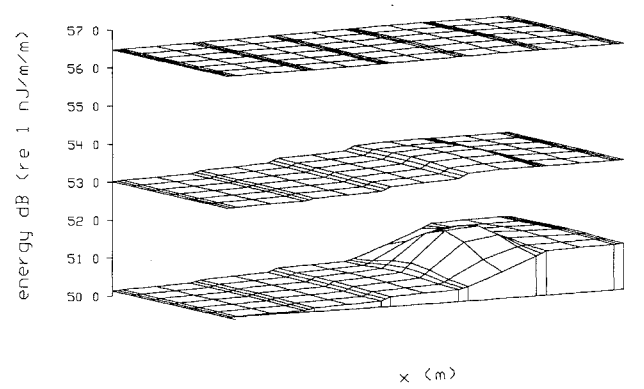

Fig. 17 Comparison of the energy density level for the plates shown in Figs. 11, 13, and 15.

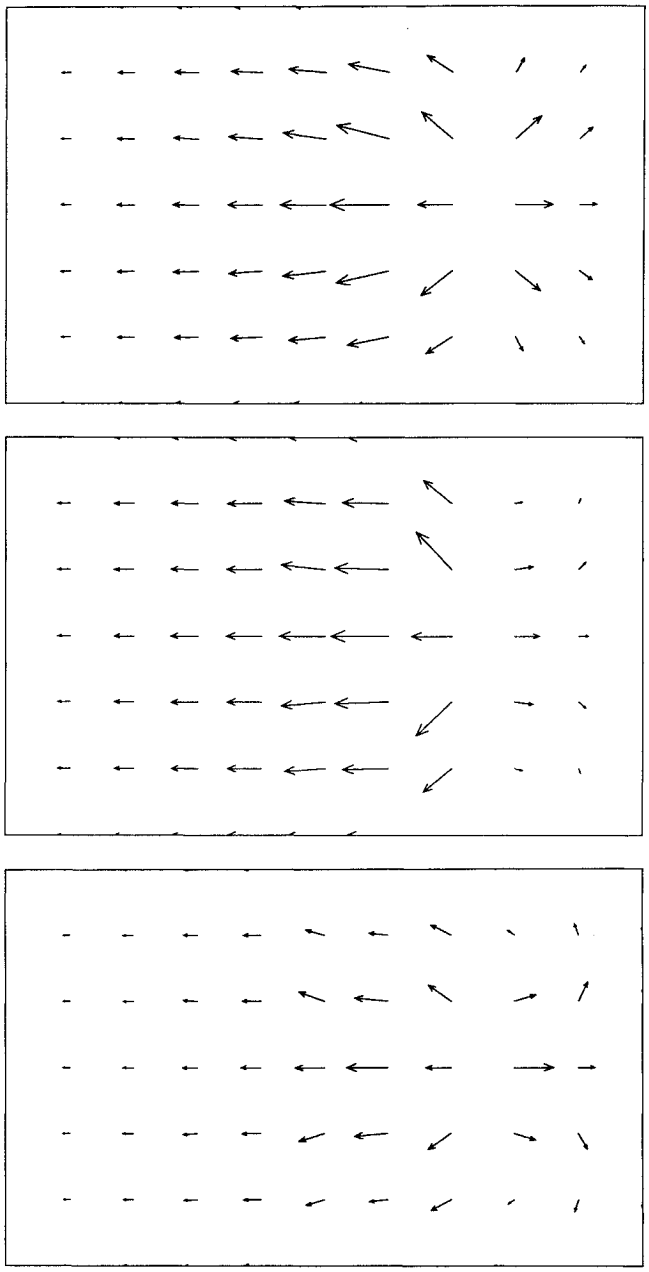

Fig. 18 Comparison of the intensity fields for the plates shown in Figs. 11, 13, and 15. The maximum vector in any of the cases above is 0.03 W/m.

fore, energy leaving the center of the plate has a tendency to come back to the outside region in order to maintain a balance of energy in the plate. As illustrated in this example, the finite element predictions can be used to make design evaluations of the best alternatives for vibration control treatments. The models also help to illustrate the phenomena that occur in cases where problems are too difficult to solve analytically.

Conclusions

Equations were derived to model the space- and time-averaged energy density and intensity in the far field of vibrating plates. The limitations and approximations of these equations have been highlighted. Verifications of Eqs. (14) and (15) were conducted to compare results with classical solutions. The results shown here are typical of the type of predicitions that can be expected using the energy equations. The smoothing effects of space averaging were especially clear in the energy density plots at low modal density.

Equations (14) and (15) were also formulated numerically and used to solve several examples. By comparing the solutions with results obtained analytically, the finite element implementations were shown to yield accurate solutions of the energy equations. The finite element method was also used to demonstrate the use of the FEM for design studies. A basic problem with some simple design parameters was used to illustrate the utility of the method. Although the predictions made by the numerical implementation of Eqs. (14) and (15) do not show much spatial variation in the energy density throughout the domain of the plate, the numerical implementation of the energy governing equations allows for some uneven distribution of the damping in the plate. The latter feature is an improvement over SEA.

The work presented in this paper is relevant to the type of problem encountered in the aerospace industry where high-frequency broadband excitations are present. Knowing the energy density and intensity fields in plates provides much insight into how energy propagates in lossy media and the strategies that can be used to control unwanted sound and vibrations.

Appendix: Expressions for Intensity and Energy

The equations below are space- and time-averaged expressions for the energy density and the intensity components in the plate. For simplicity, the following variable substitutions are used:

$$e^{--} = e^{-(\eta/2)k_{x1}x}e^{-(\eta/2)k_{y1}y} \qquad e^{+-} = e^{+(\eta/2)k_{x1}x}e^{-(\eta/2)k_{y1}y}$$

$$e^{-+} = e^{-(\eta/2)k_{x1}x}e^{+(\eta/2)k_{y1}y} \qquad e^{++} = e^{+(\eta/2)k_{x1}x}e^{+(\eta/2)k_{y1}y}$$

The energy density is

$$e = \frac{D}{4}\left[|k_x^2|^2 + |k_y^2|^2 + 2\nu k_x^2(k_y^2)^* + 2(1-\nu)|k_x k_y|^2 + \omega^2\frac{\rho}{D}\right] X(|A_1|^2|A_2|^2e^{--} + |A_1|^2|B_2|^2e^{-+} + |B_1|^2|A_2|^2e^{+-} + |B_1|^2|B_2|^2e^{++})$$

the x component of the intensity is

$$q_x = D\frac{\omega}{2}[k_x^3 + k_x k_y^2 + k_x^2 k_x^* + k_x k_y^2 + (1-\nu)k_x|k_y|^2] X(|A_1|^2|A_2|^2e^{--} + |A_1|^2|B_2|^2e^{-+} - |B_1|^2|A_2|^2e^{+-} - |B_1|^2|B_2|^2e^{++})$$

and the y component of the intensity is

$$q_y = D\frac{\omega}{2}[k_y^3 + k_y k_x^2 + k_y^2 k_y^* + k_y k_x^2 + (1-\nu)k_y|k_x|^2] X(|A_1|^2|A_2|^2e^{--} - |A_1|^2|B_2|^2e^{-+} + |B_1|^2|A_2|^2e^{+-} - |B_1|^2|B_2|^2e^{++})$$

Acknowledgment

The authors thank the Structural Acoustics Branch of the NASA Langley Research Center, which sponsored the research presented in this report through Grant NAG1-58.

References

[1]Maidanik, G., and Dickey, J., "Modal and Wave Approaches To Statistical Energy Analysis (SEA)," *Statistical Energy Analysis*, edited by K. H. Hsu, D. J. Nefske, and A. Akay, American Society of Mechanical Engineers Special Publication NCA-3, ASME, Boston,

MA, 1987, pp. 63–71.

[2]Jamshidiat, H., and SenGupta, G., "Prediction of Structural-Acoustic Response of an Aircraft Fuselage Modeled as a Periodic Structure," *Proceedings of the Twelfth Aeroacoustics Conference*, AIAA Paper 89-1045, AIAA, Washington, DC, 1989, pp. 1–13.

[3]Unruh, J. F., "Finite Element Subvolume Technique for Structural-Borne Interior Noise Prediction," *Journal of Aircraft*, Vol. 17, June, 1980, pp. 434–441.

[4]Garrelick, J. M., Cole, J. E., and Martini, K., "Structure-Borne Noise Investigations of a Twin Engine Aircraft," *Proceedings of the Tenth Aeroacoustics Conference*, AIAA Paper 86-1903, AIAA, New York, 1986, pp. 1–3.

[5]SenGupta, G., Landmann, A. E., Mera, A., and Yantis, T. F., "Prediction of Structure-Borne Noise, Based on the Finite Element Method," *Proceedings of the Tenth Aeroacoustics Conference*, AIAA Paper 86-1861, AIAA, New York, 1986, pp. 1–10.

[6]Landmann, A., and Tillema, H., "Model Size Requirements for Finite Element Prediction of Low Frequency Cabin Noise and Vibration," *Proceedings of the Twelfth Aeroacoustics Conference*, AIAA Paper 89-1076, AIAA, Washington, DC, 1989, pp. 1–5.

[7]Nefske, D. J., Wolf, J. A., and Howell, L. J., "Structural-Acoustic Finite Element Analysis of Automobile Passenger Compartment: A Review of Current Practice," *Journal of Sound and Vibration*, Vol. 80, No. 2, 1982, pp. 247–266.

[8]Lyon, R. D., *Statistical Energy Analysis*, MIT Press, Cambridge, MA, 1975, pp. 178–235.

[9]Wohlever, J. C., and Bernhard, R. J., "Energy Distribution in Rods and Beams," *Proceedings of the Twelfth Aeroacoustics Conference*, AIAA Paper 89-1122, AIAA, Washington, DC, 1989, pp. 1–9.

[10]Bouthier, O. M., Bernhard, R. J., and Wohlever, J. C., "Energy and Structural Intensity Formulations of Beams and Plate Vibrations," *Proceedings of the Third International Congress on Intensity Techniques*, Senlis, France, 1990, pp. 37–44.

[11]Lase, Y., and Jezequel, L., "Analysis of a Dynamic System Based on a New Energetic Formulation," *Proceedings of the Third International Congress on Intensity Techniques*, Senlis, France, 1990, pp. 145–150.

[12]Nefske, D. J., and Sung, S. H., "Power Flow Finite Element Analysis of Dynamic Systems: Basic Theory and Application to Beams," *Statistical Energy Analysis*, edited by K. H. Hsu, D. J. Nefske, and A. Akay, American Society of Mechanical Engineers Special Publication NCA-3, ASME, Boston, MA, 1987, pp. 47–54.

[13]Morse, P., and Ingard, U., *Theoretical Acoustics*, Princeton University Press, Princeton, NJ, 1968, pp. 199–200.

[14]Cremer, L., Heckl, M., and Ungar, E. E., *Structure-Borne Sound*, Springer-Verlag, Berlin, 1973, pp. 199–205.

[15]Noiseux, D. U., "Measurement of Power Flow in Uniform Beams and Plates," *Journal of the Acoustical Society of America*, Vol. 47, No. 1, II, 1969, pp. 238–247.

[16]Timoshenko, S., and Young, D., *Vibration Problems in Engineering*, D. Van Norstrand Co., Inc., New York, 1955, p. 442.

[17]Reddy, J. N., *An Introduction to the Finite Element Method*, McGraw Hill, New York, 1984.

[18]Zienkiewicz, O. C., *The Finite Element Method*, 3rd ed., McGraw-Hill, New York, 1977.